



## Original Article

# Chemical Stability of Conductive Ceramic Anodes in LiCl–Li<sub>2</sub>O Molten Salt for Electrolytic Reduction in Pyroprocessing

Sung-Wook Kim<sup>a,b,\*</sup>, Hyun Woo Kang<sup>a</sup>, Min Ku Jeon<sup>a,b</sup>, Sang-Kwon Lee<sup>a</sup>, Eun-Young Choi<sup>a</sup>, Wooshin Park<sup>a</sup>, Sun-Seok Hong<sup>a</sup>, Seung-Chul Oh<sup>a</sup>, and Jin-Mok Hur<sup>a</sup>

<sup>a</sup> Nuclear Fuel Cycle Process Development Group, Korea Atomic Energy Research Institute, 989-111 Daedeok-daero, Yuseong-gu, Daejeon 34057, Republic of Korea

<sup>b</sup> Department of Quantum Energy Chemical Engineering, University of Science and Technology, 217 Gajeong-ro, Yuseong-gu, Daejeon 34113, Republic of Korea

## ARTICLE INFO

## Article history:

Received 28 January 2016

Received in revised form

25 February 2016

Accepted 2 March 2016

Available online 19 March 2016

## Keywords:

Anode

Conductive Ceramics

Electrolytic Reduction

Lanthanum Strontium Manganese

Oxide

Molten Salt

Pyroprocessing

Spent Oxide Fuels

## ABSTRACT

Conductive ceramics are being developed to replace current Pt anodes in the electrolytic reduction of spent oxide fuels in pyroprocessing. While several conductive ceramics have shown promising electrochemical properties in small-scale experiments, their long-term stabilities have not yet been investigated. In this study, the chemical stability of conductive La<sub>0.33</sub>Sr<sub>0.67</sub>MnO<sub>3</sub> in LiCl–Li<sub>2</sub>O molten salt at 650°C was investigated to examine its feasibility as an anode material. Dissolution of Sr at the anode surface led to structural collapse, thereby indicating that the lifetime of the La<sub>0.33</sub>Sr<sub>0.67</sub>MnO<sub>3</sub> anode is limited. The dissolution rate of Sr is likely to be influenced by the local environment around Sr in the perovskite framework.

Copyright © 2016, Published by Elsevier Korea LLC on behalf of Korean Nuclear Society. This is an open access article under the CC BY-NC-ND license (<http://creativecommons.org/licenses/by-nc-nd/4.0/>).

## 1. Introduction

The accumulation of spent oxide fuels used in nuclear power plants has become a global issue because of their long lifetime

and radiotoxicity [1,2]. However, spent oxide fuels have several reusable radioactive species such as U, Pu, and other transuranic elements that can be recovered. Pyroprocessing is being considered as a method to manage and recycle the spent oxide

\* Corresponding author.

E-mail address: [swkim818@kaeri.re.kr](mailto:swkim818@kaeri.re.kr) (S.-W. Kim).  
<http://dx.doi.org/10.1016/j.net.2016.03.002>

1738-5733/ Copyright © 2016, Published by Elsevier Korea LLC on behalf of Korean Nuclear Society. This is an open access article under the CC BY-NC-ND license (<http://creativecommons.org/licenses/by-nc-nd/4.0/>).

fuels [3–5]. Pyroprocessing includes several electrochemical processes, such as electrolytic reduction, electrorefining, and electrowinning [3]. The spent oxide fuels can be reduced to metallic states through electrolytic reduction. Metal oxides (e.g.,  $\text{UO}_2$ ) are electrochemically dissociated into metals (e.g., U) at the cathode, and  $\text{O}_2$  gas at the anode, during electrolytic reduction using  $\text{LiCl-Li}_2\text{O}$  molten salt at  $650^\circ\text{C}$  [6]. The metal products are then recovered using electrorefining and electrowinning processes for the fabrication of the metal fuels which could be used in next-generation sodium-cooled fast reactors [3–5].

Pt is the most commonly used anode material in electrolytic reduction because of its excellent electrochemical activity and superior oxidation resistance at high temperatures (approx.  $650^\circ\text{C}$ ) [6,7]. However, the Pt anode is gradually damaged during the electrolytic reduction in the  $\text{LiCl-Li}_2\text{O}$  molten salt, owing to side reactions (e.g.,  $\text{Pt} + 3\text{O}^{2-} + 2\text{Li}^+ = \text{Li}_2\text{PtO}_3 + 4\text{e}^-$  or  $\text{Pt} = \text{Pt}^{2+} + 2\text{e}^-$ ) [6]. Additionally, Pt is one of the most expensive materials, thus alternative anode materials are needed for use in the  $\text{LiCl-Li}_2\text{O}$  molten salt system [8–12].

Conductive ceramics are potential candidates for use as  $\text{O}_2$ -evolving anode materials because of their stability in the presence of high-temperature  $\text{O}_2$  gas [8–10]. Recent studies have revealed that several conductive ceramics such as TiN,  $\text{Ni}_x\text{FeO}_y$ , and  $\text{La}_{0.33}\text{Sr}_{0.67}\text{MnO}_3$  can electrochemically reduce metal oxides to metals in the  $\text{LiCl-Li}_2\text{O}$  molten salt at  $650^\circ\text{C}$  [8–10]. However, the TiN anode significantly degrades during electrolytic reduction owing to the formation of pores, indicating its poor stability [8]. It has been claimed that  $\text{Ni}_x\text{FeO}_y$  can be chemically transformed to NiO and  $\text{Li}(\text{Ni}, \text{Fe})\text{O}_2$  at the surface (e.g.,  $\text{NiFe}_2\text{O}_4 = \text{NiO} + 2\text{LiFeO}_2$ ) during electrolytic reduction, without degradation in its electrochemical performance [9]. No noticeable phase change or physical degradation was found in the  $\text{La}_{0.33}\text{Sr}_{0.67}\text{MnO}_3$  anode after a small-scale experiment [10]. However, the long-term stability of ceramic anodes is an important issue for the scale-up of the electrolytic reducer.

In this study, we investigated the chemical stability of  $\text{La}_{0.33}\text{Sr}_{0.67}\text{MnO}_3$  to evaluate its long-term stability in the molten salt electrolyte. First,  $\text{La}_{0.33}\text{Sr}_{0.67}\text{MnO}_3$  was immersed into  $\text{LiCl-Li}_2\text{O}$  molten salt under  $\text{O}_2$  bubbling for 7 days. Its structural changes and dissolution behavior was then examined. The chemical stabilities of  $\text{SrRuO}_3$  and  $\text{LaNi}_{0.6}\text{Fe}_{0.4}\text{O}_3$ , which have similar crystal structures and elements to  $\text{La}_{0.33}\text{Sr}_{0.67}\text{MnO}_3$ , were also investigated for comparison.

## 2. Materials and methods

The chemical stability of sintered  $\text{La}_{0.33}\text{Sr}_{0.67}\text{MnO}_3$  (Toshiba Manufacturing Co., Ltd, Japan) was evaluated using 300 g of  $\text{LiCl-Li}_2\text{O}$  (1 wt.% of  $\text{Li}_2\text{O}$ ; Alfa Aesar, A Johnson Matthey Company, USA) molten salt at  $650^\circ\text{C}$ . Rectangular  $\text{La}_{0.33}\text{Sr}_{0.67}\text{MnO}_3$  (approx.  $6 \times 2.5 \times 0.6$  cm) was immersed into the molten salt (immersion depth: approx. 3 cm) and then stored for 7 days under continuous  $\text{O}_2$  bubbling (Fig. 1) to create an oxidative environment. The immersed  $\text{La}_{0.33}\text{Sr}_{0.67}\text{MnO}_3$  was rinsed with distilled water to remove any residual salt. X-ray diffraction (XRD; Bruker Corporation, D8 Advances, Germany) and energy-dispersive X-ray spectroscopy (EDS; Horiba, Ltd, X-

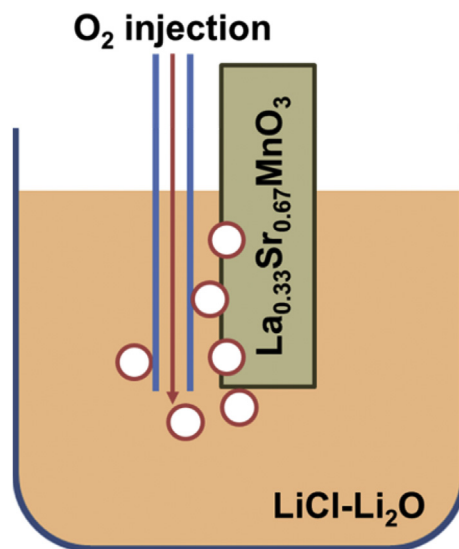


**Fig. 1** – Schematic illustration of the experimental set-up for the long-term stability test of  $\text{La}_{0.33}\text{Sr}_{0.67}\text{MnO}_3$  with  $\text{O}_2$  bubbling.

MAX, Japan) coupled with scanning electron microscopy (Hitachi, Ltd, SU-8010, Japan) were used to identify phase stability and atomic distribution before and after the immersion. Another immersion experiment was performed for 1 day (without  $\text{O}_2$  bubbling) to evaluate the cation (e.g., La, Sr, and Mn) dissolution behavior in the molten salt (3.9 g of  $\text{La}_{0.33}\text{Sr}_{0.67}\text{MnO}_3$  in 300 g of  $\text{LiCl-Li}_2\text{O}$ ). Elemental analysis of the  $\text{La}_{0.33}\text{Sr}_{0.67}\text{MnO}_3$ -immersed molten salt was performed using inductively coupled plasma-atomic emission spectroscopy (ICP-AES) to examine the cation composition of  $\text{LiCl-Li}_2\text{O}$ . Additional 1-day immersion tests were carried out on a sintered  $\text{SrRuO}_3$  (LTS Chemical Inc., USA) and  $\text{LaNi}_{0.6}\text{Fe}_{0.4}\text{O}_3$  powder (Kceracell, Co., Ltd, South Korea) for comparison.

## 3. Results and discussion

Figs. 2A and 2B show the mechanical instability of  $\text{La}_{0.33}\text{Sr}_{0.67}\text{MnO}_3$  in the  $\text{LiCl-Li}_2\text{O}$  molten salt. The surface of the sintered  $\text{La}_{0.33}\text{Sr}_{0.67}\text{MnO}_3$  was destroyed after immersion in the molten salt for 7 days under  $\text{O}_2$  bubbling. To investigate the origin of this destruction (either thermal stress or chemical reaction), the chemical stability of  $\text{La}_{0.33}\text{Sr}_{0.67}\text{MnO}_3$  before and after the immersion was examined with scanning electron microscopy-EDS and XRD (Figs. 2C and 2D). Surprisingly, no Sr was detected in several regions on the delaminated  $\text{La}_{0.33}\text{Sr}_{0.67}\text{MnO}_3$  samples (Fig. 2C), indicating that Sr was dissolved into the molten salt during the immersion. XRD patterns shown in Fig. 2D confirm the structural change of the  $\text{La}_{0.33}\text{Sr}_{0.67}\text{MnO}_3$  phase. This implies that the structural change induced by Sr dissolution is the dominant factor in the collapse of the  $\text{La}_{0.33}\text{Sr}_{0.67}\text{MnO}_3$  phase.

Pristine  $\text{La}_{0.33}\text{Sr}_{0.67}\text{MnO}_3$  possesses a well-known perovskite structure (Fig. 2D). However, it seems that the secondary phase (as indicated by the circle shown in Fig. 2D) appeared around the original peaks during the immersion, and the

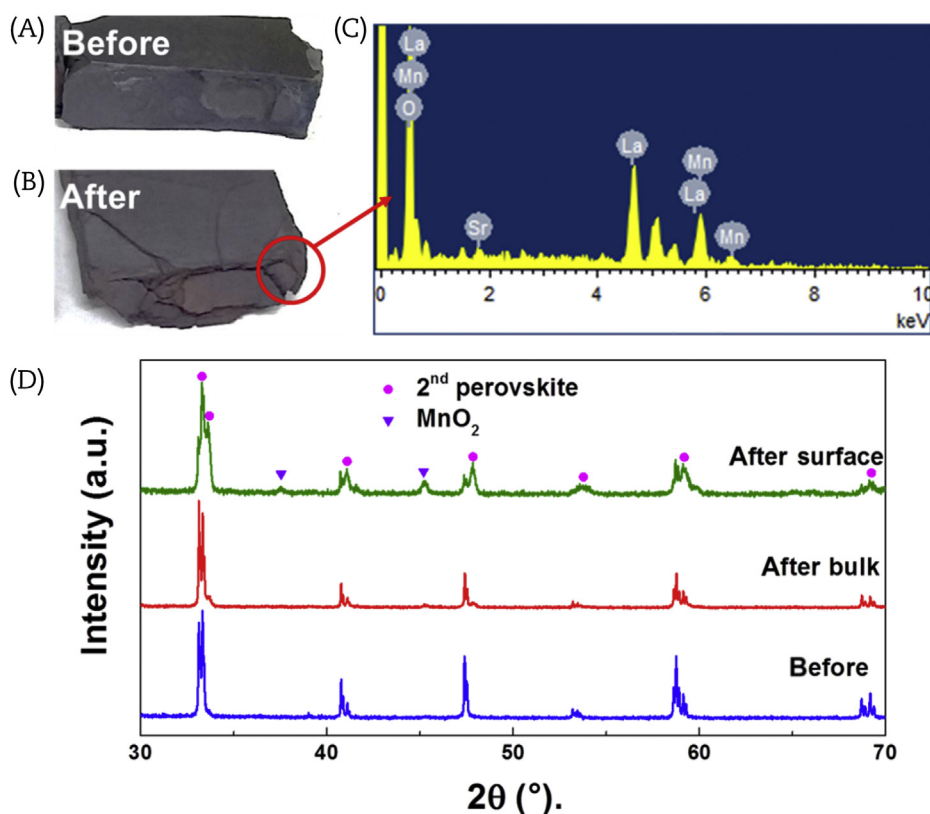


**Fig. 2** – Photographs of sintered  $\text{La}_{0.33}\text{Sr}_{0.67}\text{MnO}_3$ . (A) Before immersion in  $\text{LiCl-Li}_2\text{O}$  for 7 days with  $\text{O}_2$  bubbling. (B) After immersion in  $\text{LiCl-Li}_2\text{O}$  for 7 days with  $\text{O}_2$  bubbling. (C) Energy dispersive X-ray spectroscopy result of the delaminated region in immersed  $\text{La}_{0.33}\text{Sr}_{0.67}\text{MnO}_3$ . (D) X-ray diffraction patterns of  $\text{La}_{0.33}\text{Sr}_{0.67}\text{MnO}_3$  before and after immersion. a.u., arbitrary unit.

intensity of the secondary peaks became higher in the delaminated area, compared with that in the bulk area after the immersion. Hence, it is thought that the phase change is more favored near the surface, leading to the collapse of  $\text{La}_{0.33}\text{Sr}_{0.67}\text{MnO}_3$  at the surface. The overall diffraction pattern of the secondary phase resembles that of the pristine materials, suggesting a similar crystal structure of the secondary phase to the original one. Hence, the secondary phase is believed to be the off-stoichiometric perovskite-like  $\text{La-Mn-O}$  phase (Sr-free/deficient). In addition, a third phase (as indicated by the reverse-triangle shown in Fig. 2D), whose peak position does not match that of the perovskite, can be seen after the immersion. This phase is likely to be  $\text{MnO}_2$  (PDF#42-1169), which can be formed owing to the presence of excess Mn compared with La.

The cation dissolution behavior of  $\text{La}_{0.33}\text{Sr}_{0.67}\text{MnO}_3$  was quantitatively studied using ICP-AES, as summarized in Table 1. After a 1-day immersion (without  $\text{O}_2$  bubbling), 128 ppm of

Sr were detected in the molten salt, while compositions of La and Mn were not less than the detection limit. This result agrees with the EDS analysis, demonstrating the dissolution behavior of Sr (Fig. 2C). The amount of dissolved Sr in  $\text{LiCl-Li}_2\text{O}$  was approximately 0.038 g, while that in the pristine material was approximately 1.10 g (approx. 3.45% loss per day). Such a dissolution rate is likely to be problematic for long-term use of  $\text{La}_{0.33}\text{Sr}_{0.67}\text{MnO}_3$  (simply, approx. 50% loss after 20 days).

For comparison, the dissolution behavior of a Sr-rich perovskite,  $\text{SrRuO}_3$ , was studied. The sintered  $\text{SrRuO}_3$  was completely lost and a powdered product was obtained after the immersion, as shown in Figs. 3A and 3B. The XRD data depicted in Fig. 3C clearly shows that the  $\text{SrRuO}_3$  phase was eliminated during the immersion to form a metallic Ru phase. This means that the dissolution rate of Sr in  $\text{SrRuO}_3$  is much faster than that in  $\text{La}_{0.33}\text{Sr}_{0.67}\text{MnO}_3$ . Therefore, the dissolution behavior of Sr is not solely affected by the Sr element itself, but is also strongly related to the local environment surrounding Sr.

The chemical stability of the Sr-free perovskite compound,  $\text{LaNi}_{0.6}\text{Fe}_{0.4}\text{O}_3$ , was also investigated, as shown in Fig. 4 and Table 1. Despite the absence of Sr in the  $\text{LaNi}_{0.6}\text{Fe}_{0.4}\text{O}_3$  structure, a more severe structural degradation occurred compared with that seen in  $\text{La}_{0.33}\text{Sr}_{0.67}\text{MnO}_3$  (Fig. 4). ICP-AES analysis showed that both Ni and Fe were soluble in the  $\text{LiCl-Li}_2\text{O}$  molten salt, as shown in Table 1. La composition was less than

**Table 1** – Summary of the inductively coupled plasma-atomic emission spectrometry results of the  $\text{LiCl-Li}_2\text{O}$  molten salt after immersion of  $\text{La}_{0.33}\text{Sr}_{0.67}\text{MnO}_3$  and  $\text{LaNi}_{0.6}\text{Fe}_{0.4}\text{O}_3$  for 1 day each (unit: ppm).

Element	La	Mn	Sr	Ni	Fe
$\text{La}_{0.33}\text{Sr}_{0.67}\text{MnO}_3$	N/A	N/A	~128	–	–
$\text{LaNi}_{0.6}\text{Fe}_{0.4}\text{O}_3$	N/A	–	–	~10	~10

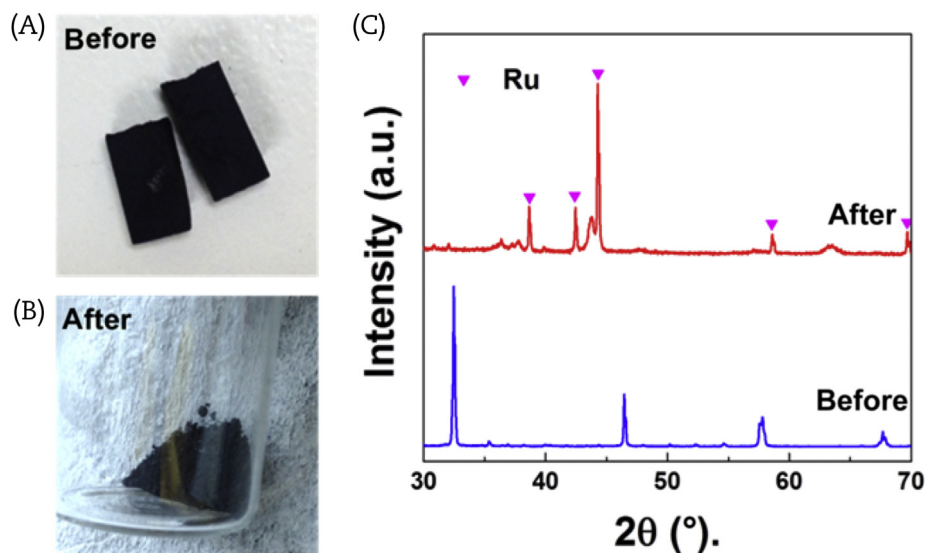


Fig. 3 – Photographs of sintered  $\text{SrRuO}_3$ . (A) Before immersion in  $\text{LiCl-Li}_2\text{O}$  for 1 day. (B) After immersion in  $\text{LiCl-Li}_2\text{O}$  for 1 day. (C) The corresponding X-ray diffraction pattern. a.u., arbitrary unit.

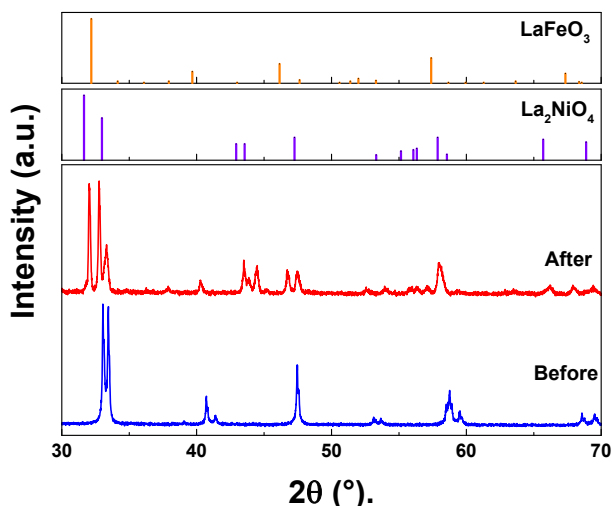


Fig. 4 – X-ray diffraction patterns of  $\text{LaNi}_{0.6}\text{Fe}_{0.4}\text{O}_3$  before and after immersion in  $\text{LiCl-Li}_2\text{O}$  for 1 day. a.u., arbitrary unit.

the detection limit after the immersion, similar to  $\text{La}_{0.33}\text{Sr}_{0.67}\text{MnO}_3$ , implying a high stability of La in  $\text{LiCl-Li}_2\text{O}$ . It is interesting that the structural change of  $\text{LaNi}_{0.6}\text{Fe}_{0.4}\text{O}_3$  is more drastic than that of  $\text{La}_{0.33}\text{Sr}_{0.67}\text{MnO}_3$  in spite of the lesser amount of Ni/Fe dissolution. This probably occurred because  $\text{LaNi}_{0.6}\text{Fe}_{0.4}\text{O}_3$  separated into Ni-rich ( $\text{La}_2\text{NiO}_4$ -like) and Fe-rich ( $\text{LaFeO}_3$ -like) phases. It is thought that the perovskite  $\text{LaNi}_{0.6}\text{Fe}_{0.4}\text{O}_3$  phase cannot be stabilized, even with a small amount of cation dissolution.

#### 4. Conclusion

Chemical stabilities of conductive ceramics ( $\text{La}_{0.33}\text{Sr}_{0.67}\text{MnO}_3$ ,  $\text{SrRuO}_3$ , and  $\text{LaNi}_{0.6}\text{Fe}_{0.4}\text{O}_3$ ) in the  $\text{LiCl-Li}_2\text{O}$  molten salt were

investigated to examine their feasibility as long-term stable anode materials in electrolytic reduction. Cation dissolution (e.g., Sr, Ni, and Fe) is a dominant factor affecting the chemical instability of these compounds. It seems that the dissolution rate of the cations varies depending on the local environment as well as the type of the elements. La and Mn remained stable in the perovskite structure in the  $\text{LiCl-Li}_2\text{O}$  molten salt. Hence, the Sr-free/deficient La-Mn-O phase may be promising as a long-lasting anode material, but its electrical conductivity, electrochemical activity, and mechanical stability should be considered.

#### Conflicts of interest

All authors have no conflicts of interest.

#### Acknowledgments

This work was supported by the National Research Foundation of Korea grant, funded by the Korea government (MISP; 2012M2A8A5025697).

#### REFERENCES

- [1] C. Braun, R. Forrest, Considerations regarding ROK spent nuclear fuel management options, *Nucl. Eng. Technol.* 45 (2013) 427–428.
- [2] L.B. Silverio, W.D.Q. Lamas, An analysis of development and research on spent oxide fuel reprocessing, *Energy Policy* 39 (2011) 281–289.
- [3] H.-S. Lee, G.-I. Park, K.-H. Kang, J.-M. Hur, J.-G. Kim, D.-H. Ahn, Y.-Z. Cho, E.-H. Kim, Pyroprocessing technology development at KAERI, *Nucl. Eng. Technol.* 43 (2011) 317–328.
- [4] H. Ohta, T. Inoue, Y. Sakamura, K. Kinoshita, Pyroprocessing of light water reactor spent fuels based on an

- electrochemical reduction technology, *Nucl. Technol.* 150 (2005) 153–161.
- [5] T. Inoue, L. Koch, Development of pyroprocessing and its future direction, *Nucl. Eng. Technol.* 40 (2008) 183–190.
- [6] S.M. Jeong, H.-S. Shin, S.-H. Cho, J.-M. Hur, H.S. Lee, Electrochemical behavior of a platinum anode for reduction of uranium oxide in a LiCl molten salt, *Electrochim. Acta* 54 (2009) 6335–6340.
- [7] J.-M. Hur, S.M. Jeong, H.S. Lee, Underpotential deposition of Li in a molten LiCl–Li<sub>2</sub>O electrolyte for the electrochemical reduction of U from uranium oxides, *Electrochem. Commun.* 12 (2010) 706–709.
- [8] S.-W. Kim, E.-Y. Choi, W. Park, H.S. Im, J.-M. Hur, TiN anode for electrolytic reduction of UO<sub>2</sub> in pyroprocessing, *J. Nucl. Fuel Cycle Waste Technol.* 13 (2015) 229–233.
- [9] Y. Sakaumra, M. Iizuka, Applicability of nickel ferrite anode to electrolytic reduction of metal oxides in LiCl–Li<sub>2</sub>O melt at 923 K, *Electrochim. Acta* 189 (2016) 74–82.
- [10] S.-W. Kim, E.-Y. Choi, W. Park, H.S. Im, J.-M. Hur, A conductive oxide as an O<sub>2</sub> evolution anode for the electrolytic reduction of metal oxides, *Electrochem. Commun.* 55 (2015) 14–17.
- [11] A. Merwin, D. Chidambaram, Alternative anodes for the electrolytic reduction of UO<sub>2</sub>, *Metall. Mater. Trans. A* 46 (2015) 536–544.
- [12] S.-W. Kim, W. Park, H.S. Im, J.-M. Hur, S.-S. Hong, S.-C. Oh, E.-Y. Choi, Electrochemical behavior of liquid Sb anode system for electrolytic reduction of UO<sub>2</sub>, *J. Radioanal. Nucl. Chem.* 303 (2015) 1041–1046.